

Alma Mater Studiorum Università di Bologna  
Archivio istituzionale della ricerca

Control-Oriented Exhaust Gas Temperature Modelling Based on Wiebe Equation

This is the final peer-reviewed author's accepted manuscript (postprint) of the following publication:

*Published Version:*

Mecagni J., Brusa A., Cavina N., Corti E., Silvestri N., Cucchi M. (2021). Control-Oriented Exhaust Gas Temperature Modelling Based on Wiebe Equation. SAE INTERNATIONAL JOURNAL OF ENGINES, 14(5), 697-712 [10.4271/03-14-05-0042].

*Availability:*

This version is available at: <https://hdl.handle.net/11585/840233> since: 2024-05-14

*Published:*

DOI: <http://doi.org/10.4271/03-14-05-0042>

*Terms of use:*

Some rights reserved. The terms and conditions for the reuse of this version of the manuscript are specified in the publishing policy. For all terms of use and more information see the publisher's website.

This item was downloaded from IRIS Università di Bologna (<https://cris.unibo.it/>).  
When citing, please refer to the published version.

(Article begins on next page)

# Control-Oriented Exhaust Gas Temperature Modelling based on Wiebe Equation

Author, co-author (Do NOT enter this information. It will be pulled from participant tab in MyTechZone)

Affiliation (Do NOT enter this information. It will be pulled from participant tab in MyTechZone)

## Abstract

Exhaust gas temperature is one of the main parameters under engine manufacturers' focus, due to its effects on both Turbo-Charger durability and catalyst efficiency. Typically, the measurement of such variable at the test bench is carried out by using thermocouples, which are not available for on-board application. For this reason, an accurate and reliable model for Real-Time (RT) calculation of this variable is particularly important.

In this work a control-oriented model for the estimation of exhaust temperature in Spark Ignition (SI) engines is developed and validated exploiting experimental data. A fundamental quantity that has to be necessarily known is the temperature of the gas within the exhaust manifold or at the exhaust valves opening. The first part of this paper deals with the development of a 0-D combustion model, identifying the main parameters of the Wiebe function with an automatic optimization routine. Such method allows to accurately reproduce the in-cylinder pressure trace and calculate the temperature of the gas at exhaust valve opening. Hence, an analytical function that converts such temperatures into the exhaust manifold ones is developed by analyzing the experimental measurements of thermocouples installed in the exhaust manifold under steady state operating conditions. This is the main reason why the proposed approach cannot be considered fully empirical.

The resulting zero-dimensional model is not suitable for a RT application, nor to be implemented in an Engine Control Unit (ECU) due to a differential equation that needs to be solved in the angular domain. For this reason, in the second part of the paper a control-oriented model is developed by using an analytical methodology, which exploits the combustion model and the temperature analytical function presented in the first part. Finally, the control-oriented model is coupled with a thermocouple (TC) dynamics RT model and both are validated under transient conditions.

**Keywords:** combustion, modelling, Wiebe, exhaust, temperature turbine, thermocouple, control-oriented

## Introduction

Increasingly stringent regulations on pollutants production and CO<sub>2</sub> reduction are forcing manufacturers to improve combustion and three-way catalyst conversion efficiency in SI engines. Engine operation with stoichiometric mixture on the entire operating range is considered as the most robust solution to achieve both goals, but in modern downsized turbocharged SI engines such aim is not reachable mainly due to the maximum allowed temperature admissible at the

turbine inlet. Indeed, mixture enrichment and load reduction are the commonly adopted strategies to mitigate exhaust temperature, in order to prevent turbine damage, as well explained in [1]. It is also fundamental to reach the optimal temperature of the three-way catalyst as fast as possible during cold starts for an efficient conversion of pollutants emissions. Spark Advance (SA) degradation is the most common strategy to reach a poorer combustion efficiency and a higher exhaust gas temperature, as described in [2]. Hence, control-oriented models implemented in ECU that can accurately estimate the exhaust gas temperature on the entire engine operating field are a strategic tool to prevent turbine failure and maximize the conversion efficiency of the after-treatment system, as highlighted by Fu and Chen [3]. Nevertheless, few examples of RT models able to estimate the inlet turbine temperature are present in literature. One of the available studies is proposed by Fulton and Van Nieuwstadt [4], who describe an algorithm for the estimation of gas temperature at turbine inlet, which is composed of an open loop model and a closed loop contribution (based on a PI controller) which corrects the output of the open loop chain according to the TC signal mounted at the turbine outlet. However, TCs or other sensors such as Resistance Temperature Detectors (RTDs) are not used for the final on-vehicle application for cost and reliability reasons. Therefore, other methods have been implemented in order to estimate exhaust temperature, exploiting production sensors such as UEGO ones. Indeed, heaters of *lambda* sensors can be used to evaluate exhaust gas temperature by analyzing the shape of the duty cycle signal, with which current flux to the heating element is controlled in order to compensate the effect of the surrounding exhaust gas on the measurement [5]. Electrical heating power is then a function of its own temperature: this means that the exhaust gas temperature can be estimated based on the relationship between these two values. Thus, considering currently available sensors for on-board applications, it is not possible to directly measure the gas temperature at turbine inlet, but it can be just estimated and this confirms the importance of an accurate model for the calculation of such parameter.

The focus of this work is the development of a semi-physical simulation-oriented model for the calculation of the exhaust temperature at turbine inlet that can be directly converted into a control-oriented algorithm, that is suitable for the cycle-by-cycle calculation of some combustion indexes and for the implementation in a development ECU. The temperature of the exhaust gases at Exhaust Valve Opening (EVO) is considered as the starting point from which the corresponding value at the turbine inlet can be evaluated. For this reason, in the first part of the paper, a Wiebe-based combustion model is developed to reproduce the mean in-cylinder pressure trace for the closed valves portion of the engine cycle, through the implementation of a modified heat release equation and a calibrated heat transfer model [6], in a 0-D simulation environment (Simulink). Wiebe equation is a standard approach to

simulate combustion heat release in SI and Compression Ignition (CI) engines and nowadays it is mainly used to develop RT models for Software-in-the-Loop (SiL) and Hardware-in-the-Loop (HiL) systems. Some authors also exploit such method to study autoignition cycles [7]. In the field of SiL and HiL oriented models, Saad et al. [8] developed a CI engine model based on Wiebe law, compatible with the implementation in a RT target machine. Nevertheless, combustion parameters are calibrated just for a limited portion of engine operating field and such observation demonstrates the intrinsic difficulty in identifying proper values of the equation parameters with a RT-compatible methodology. Considering SI engines, Malbec et al. [9] calibrated a phenomenological combustion model for a limited number of operating conditions and then extended the experimental database with a Neural-Network (NN) approach. In this way it is possible to calibrate a control-oriented combustion model, in which heat release is reproduced by implementing a function comparable with Wiebe law. In literature, standard Wiebe function is not only applied to develop engine models compatible with RT applications but even to define on board algorithms for the estimation of some synthetic combustion indexes. Ravaglioli et al. [10] describe a RT-compatible Wiebe-based model for the estimation of combustion phase in CI engines. Considering the applications described above, one of the main contributions of the paper is the optimization routine that is used to identify the optimal Wiebe parameters on the entire engine operating range, when experimental indicating data and ECU indexes are available. For these reasons, in this work the trend in the values of the optimized Wiebe coefficients is analyzed as a function of engine speed, load, and spark timing (all experimental conditions are tested with calibrated, and pre-fixed, lambda values) in order to develop an analytical model based on polynomial functions according to the approach explained in [11] and [12]. The procedure described allows the identification of a method to analytically define the trend over engine speed and load axes of the Wiebe function parameters with high accuracy: the approach can be considered innovative because in this way the resulting model is actually suitable for RT applications and it can be directly implemented in an ECU for the estimation of main combustion indexes. Moreover, model coefficients calibrated for a completely different kind of engine are compared with values obtained for engine used for model development and validation to demonstrate the reliability and the general validity of the proposed analytical approach.

Polynomials used for the calculation of Wiebe equation coefficients are an extremely powerful way to calibrate related maps that are implemented in the ECU. Numerical maps and basic logical operations represent indeed the only way to implement algorithms in the commercial control units and to avoid calculations that implies, for instance, a relevant optimization effort for the binary representation of the inputs and outputs of each function (such as the power function). At the same time, once the type of the coefficient function is known, the analytical method allows to significantly reduce the experimental campaign for the calibration process, w.r.t. the effort needed by the identification of a map. Moreover, while a polynomial can be easily reversed to use output as inputs and vice versa, the same is not possible for a numerical map. An alternative approach to calculate the coefficients of the Wiebe law as function of the operating conditions is that to use neural networks. This method is proposed, also, in GT-Power software [13] and it is labelled as "Semi-Predictive" approach. Egan et al. [14] explain how the combustion control systems based on neural networks can well capture the non-linearity of the controlled system and the execution time of such algorithms can be compatible with a RT execution.

Nevertheless, they have tested these models on a PC and not on a development ECU that effectively controls engine actuators.

Once the combustion model calibration process is concluded, the gas temperature within the combustion chamber at EVO can be calculated for all engine points. Such parameter allows to estimate the gas temperature within the exhaust manifold with physical approaches based on the solution of Partial Differential Equations (PDE) or lumped models [15]. Both cited methods need data about engine geometry, such as exhaust valves lift or thickness of the exhaust manifold walls. In this case geometrical features of studied engine are not available, so an empirical function is defined to convert the simulated temperature at EVO into the value measured at turbine inlet: the implementation of such analytical model coupled with a physical combustion one motivates the label "semi-physical" for the proposed approach. The temperature analytical function, calibrated by exploiting the experimental measurements under steady state conditions of the TC placed at the turbine inlet, includes all the heat exchange effects due to convection, conduction and radiation phenomena between the combustion chamber and the considered location. Also in this case, the analytical approach is the solution to make this calculation compatible with the implementation in a production control strategy. In order to measure the exhaust temperatures, standard Mineral Insulated Metal Sheathed (MIMS) TCs are used. Thermocouple temperature measurements under steady state conditions are underestimated with respect to the real values, due to radiation and conduction heat transfer effects between pipe wall and TC, and along the sensor body itself. The latter is due to the temperature gradient on the TC body, and it has a higher influence on the measured temperature value with respect to radiation [16], that can thus be considered as negligible. Despite the influence of these phenomena for steady state measurements, thermocouples are used by many manufacturers in order to define the maximum temperatures that components like turbine and three-way catalyst can withstand. Thus, an exhaust gas temperature model calibrated with TC values can be considered reliable when used to control gas temperature at the turbine inlet, because temperature limits for exhaust systems are defined by component suppliers using the same type of sensor (and this is also true for the so-called catalyst activation temperature).

The resulting calibrated semi-physical model is particularly useful for the development of control systems which use spark timing to manage exhaust temperature, because it can be directly adapted for the implementation in a development ECU. However, when the final objective is that to develop a control-oriented algorithm, the 0-D approach cannot be directly used to calculate cycle-by-cycle combustion indexes because an energy balance equation needs to be solved in the angular domain. Muric et al. [17] propose a fast crank angle resolved 0-D combustion model to estimate the NO<sub>x</sub> production cycle-by-cycle, but this solution requires an embedded hardware equipped with dedicated Field Programmable Gate Array (FPGA) circuits. FPGA is available on modern controller units, but it is usually dedicated to acquire and generate signals, control the actuators and manage communications protocols and ports. Hence, the execution effort needed by the model must be inevitably rationalized for the implementation on production ECUs. For such reason, the analytical approach is the strategic solution to meet the constraints imposed by the computational power available on the final implementation in production control units.

In the last part of the paper the real-time algorithm is validated by comparing the simulated exhaust temperature and 50% Mass Fuel Burned (MFB50) profiles with the experimental ones recorded at the test bench operating the engine under transient conditions, also

considering the dynamic response of the thermocouple. Thus, the exhaust temperature model is coupled with a TC dynamic control-oriented one. TC behavior is affected by convective, conduction and radiation phenomena described above but even by sensor thermal inertia. Indeed, TC temperature cannot follow changes in gas temperature instantaneously due to its finite mass [18]. Sensor behavior under transient conditions is directly related to the time constant which is defined by Equation (1):

$$\tau = \frac{m k_p}{A h} \quad (1)$$

Where  $m$  is the mass,  $k_p$  is the heat capacity,  $A$  is the surface area and  $h$  the convective heat transfer coefficient. Therefore, the time constant is affected by design parameters and by the flow field characteristics. In literature, the most common approaches used to simulate the transient effect on thermocouple measurements are based on Kalman filters [19], and on exponential Moving Average (MA). The second method for TC dynamics simulation is proposed in this paper and it was described by the authors in a previous work [20]. It includes two MAs that were calibrated to reproduce the resulting trend of the TC signal, as measured during transient tests.

## Experimental Setup

The experimental tests were carried out on a V8, 3.9-L, GDI, Turbo-Charged engine, in which a piezoelectric sensor is installed inside each cylinder and a thermocouple is mounted at the turbine inlet. More features of such engine are reported in Table 1.

Table 1. Engine characteristics.

Displaced volume	3.9 L (8 cylinder) - turbo
Stroke	82 mm
Accuracy	86.5 mm
Connecting Rod	143 mm
Compression ratio	9.45:1
Number of Valves per Cylinder	4
Spark-plug position	central
Injector position	lateral

Data used for the development of the model have been recorded on engine points that cover the entire operating range. High engine speed and load points are the most important operating conditions because it is the area where the mixture enrichment would be adopted to prevent turbine failure. Figure 1 shows such points in the engine speed-load field. Data are normalized with respect to their maximum value for confidentiality reasons.

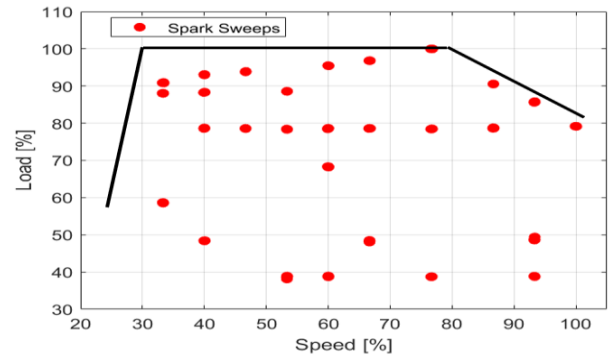


Figure 1. Explored engine points regarding speed and load, where spark sweeps are carried out.

For each steady state condition shown in Figure 1, a spark sweep is performed to change the combustion phase, while maintaining fixed other actuations, for a total of about 150 different operating conditions. For each SA value, in-cylinder pressure signals are recorded for 200 consecutive cycles with a sampling frequency of 200 kHz by using Alma Automotive OBI system. From all these traces, the combustion indexes are then calculated: in particular, the MFB10, MFB50 and MFB90 are obtained from the Cumulative Net Heat Release, calculated by exploiting the low-pass-filtered pressure curves, with a polytropic index equal to 1.32 [21]. The combustion model introduced above is developed in order to simulate the mean pressure curve, thus experimental low-pass-filtered, in-cylinder pressure signals are used to calculate the mean pressure trace between all cylinders for each operating condition defined by engine speed, load (identified with a specific ECU index related to the trapped air mass) and SA.

The exhaust gas temperature is measured with a thermocouple directly exposed to the exhaust gases, that is installed at the turbine inlet of each engine bank. The measurement chain of such signal is composed by a National Instrument Compact-Rio 9024, on which the specific module 9213 is mounted, and the sampling frequency is equal to 100 Hz. Such characteristic of the measurement chain is enough for the development of the exhaust gas temperature model because it is based on steady-state measurements performed during spark sweep tests. Indeed, the thermocouple value is recorded for 10 seconds for each operating condition and then they are averaged to obtain the exhaust gas temperature for given engine speed, load, and SA.

In the following table main features of the thermocouple installed on the exhaust system are summarized.

Table 2. Thermocouple characteristics.

Type	K
Diameter	3 mm
Accuracy	$\pm 2.2 \text{ }^{\circ}\text{C}$

During spark sweep tests, all other sensors installed on the engine were recorded with a sampling frequency of 100Hz. Finally, some tests characterized by transient conditions are carried out, while recording combustion indexes and TC outputs. Such tests were performed mainly to validate the control-oriented model under transient conditions.

## Semi-Physical Model

The semi-physical model is mainly composed of two parts. The first one includes a Wiebe-based combustion model, with a Woschni wall heat transfer model previously calibrated in GT Power, which allows to calculate the in-cylinder pressure curve between the Intake Valve Closing (IVC) and the EVO. The engine under test has a Variable Valve Timing (VVT) system, thus, in order to be sure to analyze the closed valves portion of the cycle only, it is decided to perform the calculation of the in-cylinder pressure curve in the range between 60 CA° Before firing Top Dead Center (BTDC) and 140 CA° After firing Top Dead Center (ATDC). It is important to highlight that the temperature calculated at 140 CA° ATDC is considered as the EVO value. The second part of the model implements an analytical transfer function with which it is possible to calculate the gas temperature at the turbine inlet, starting from the corresponding value within the combustion chamber at EVO, as calculated with the combustion model.

The calibration of the combustion model is carried out by exploiting the fuel consumption data and the lambda measurements, with which it is possible to estimate the air mass trapped into the cylinder, and the experimental pressure traces. Using simulated temperature values within the combustion chamber at EVO, and the measured ones at the turbine inlet under steady-state conditions, the transfer function is then calibrated.

The scheme of the semi-physical model implemented in Simulink is shown in the following figure. Inputs of the first block are engine speed, load and SA. It is important to mention that lambda is not an input of the combustion model because the calibration is performed with experimental data only, with base (mapped) lambda values. Nevertheless, the lambda map is implemented in the model because it is needed to calculate the stoichiometric mass of fuel, which reacts during the combustion process. With the simulated MFB50, engine speed and load, the second block calculates the offset value to convert the gas temperature at EVO into the value recorded at the turbine inlet under steady-state conditions.

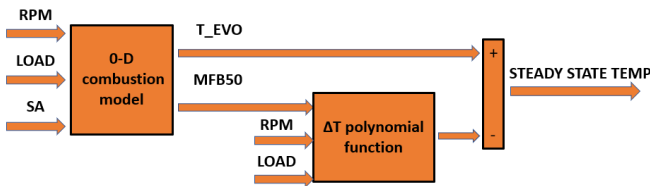


Figure 2. Layout of the semi-physical simulation-oriented model. The inputs are engine speed, load and SA.

## 0-D combustion model

The 0-D combustion model is developed considering the energy balance for a closed system. Equation (2) allows to calculate the infinitesimal temperature variation within the combustion chamber:

$$dT = \frac{dQ_{comb} - dQ_{wall} - pdV}{c_v M} \quad (2)$$

Where:

- $dQ_{comb}$  is the infinitesimal energy introduced within the cycle during the combustion process. This contribution is not modelled with the classical Wiebe function but with the version implemented in GT-Power software [6]:

$$\chi(\vartheta) = 1 - \exp(-WC(\vartheta - SOC)^{E+1}) \quad (3)$$

In which  $\vartheta$  is the current crank angle value, E is the Wiebe exponent, SOC represents the start of combustion and WC is the efficiency parameter. According to the GT-Power software, such coefficient can be calculated with the following equation:

$$WC = \left( \frac{D}{\frac{1}{BEC^{E+1}} - \frac{1}{BSC^{E+1}}} \right)^{-(E+1)} \quad (4)$$

Where D is the combustion duration,  $BEC = -\ln(0.1)$  and  $BSC = -\ln(0.9)$

- $dQ_{wall}$  is the infinitesimal energy loss towards the walls of the combustion chamber and it was modelled with a calibrated Woschni formula
- $pdV$  represents the infinitesimal work
- $M$  is the total mass trapped into the cylinder
- $c_v$  is the specific heat at constant volume. The gas inside the combustion chamber is considered as a mixture of perfect gases as oxygen, nitrogen, vaporized fuel, carbon dioxide and water vapor (with the last two species that are generated during combustion). This means that  $c_v$  can be expressed as weighted average of the  $c_{v-i}$  of each gas [22]. It is important to consider the dependency with temperature of the specific heat at constant volume and pressure. This trend is modelled exploiting the Janaf tables [23] which allow to calculate the specific heat at constant pressure of a certain chemical species. By knowing  $c_{p-i}$  it is possible to calculate  $c_{v-i}$  via the perfect gas hypothesis. The same hypothesis allows the conversion of the calculated temperature into the corresponding pressure value

Equation (2) can be integrated in order to determine the temperature profile on the closed valves portion of the cycle, but the initial temperature is needed. This can be calculated with the perfect gas law by knowing the initial pressure, obtained from the experimental pressure curves for a certain crank angle value within the compression phase (60 CA° BTDC in this work), the corresponding cylinder volume, and the trapped air mass (as calculated from the fuel consumption data and lambda measurements). Initial pressure and the trapped mass of air were implemented in the 0-D model with polynomial equations with engine speed and load as independent variables, as shown in Figure 3.

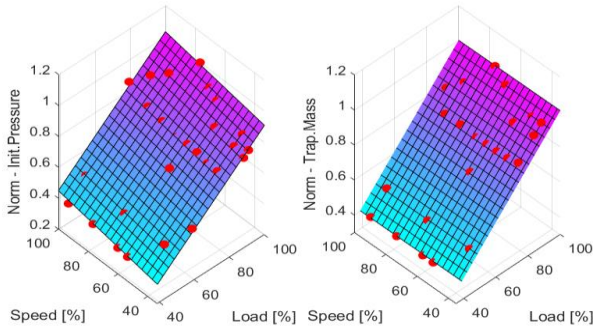


Figure 3. Normalized pressure in the combustion chamber at 60° CA BTDC and normalized trapped mass as a function of engine speed and load. Red dots represent the experimental values.

The output of the surface shown in the subplot on the right allows to calculate the stoichiometric mass of fuel, which reacts during the combustion, and the injected mass of fuel using the output of the lambda target map.

The calibration of the combustion model consists of the identification of the optimal values of coefficients E and D (Equations (3) and (4)), when setting the SOC equal to SA. An automatic algorithm is developed in Matlab to identify the best Wiebe parameters for each operating condition characterized by engine speed, load and SA. The optimization routine has the purpose of minimizing the objective function ( $fo$ ) defined as the mean absolute error between the experimental pressure trace and the simulated one. Equation (5) represents the mathematical formulation of the objective function:

$$fo = \sum_{i=1}^n \frac{|p_{exp}(i) - p_{sim}(i)|}{n} \quad (5)$$

In which  $n$  is the number of samples, directly correlated to the angular step used during the simulation (0.1 CA° in this work). Figure 4 displays on the left a normalized pressure curve after the calibration process and on the right the corresponding normalized energy balance, for the engine point 2500 RPM, full load. In the subplot on the right  $Q_c$  represents the gross heat release, while  $Q_w$  the heat loss towards the walls of the combustion chamber. Instead,  $W$  is the indicated work and  $E$  the internal energy.

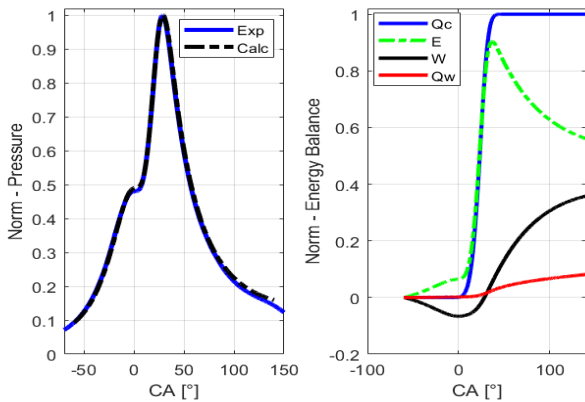


Figure 4. Calculated and experimental mean in-cylinder pressure curve are displayed on the left, while the energy balance is shown on the right.

In the plot on the left of Figure 5, the values of the objective function at the end of the calibration process are shown for all the tested points. Mean absolute error between experimental and simulated pressure trace is under 1 bar for 92% of tests. Thus the calibration process is considered as positively concluded. On the right it is reported the analysis on cumulative heat release curves: in particular, applying the Equation (5) to the experimental and simulated heat release curves, it is possible to calculate the mean absolute error between such quantities. Considering that the values are always under 70 J (that is equivalent to 3%) it is possible to conclude that the model simulates with high accuracy the heat release (and consequently the pressure trace) for all the tested points.

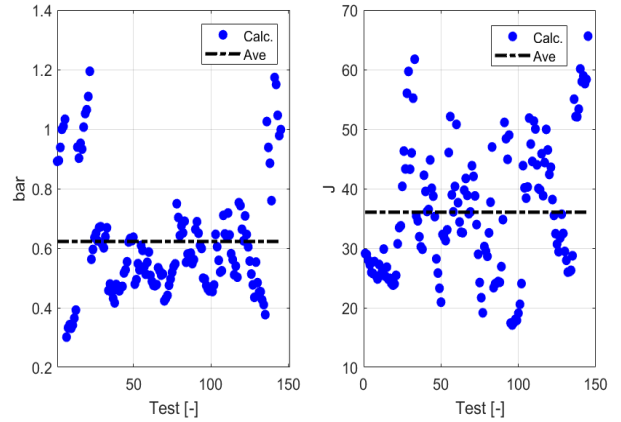


Figure 5. Absolute mean error between the experimental and simulated pressure traces and cumulative heat release for each tested engine point at the end of the calibration process.

Even the simulated heat release is compared with the experimental one. The comparison is carried out for combustion indexes such as MFB50 and combustion duration (defined as the difference between MFB90 and MFB10) in order to simplify the process. Values were normalized to highlight that all points and fitting lines are close to the bisector of the plotting grid. Figure 6 also displays R-Square ( $R^2$ ) and Root Mean Square Error (RMSE) indexes that were calculated with the corresponding Matlab functions [24].

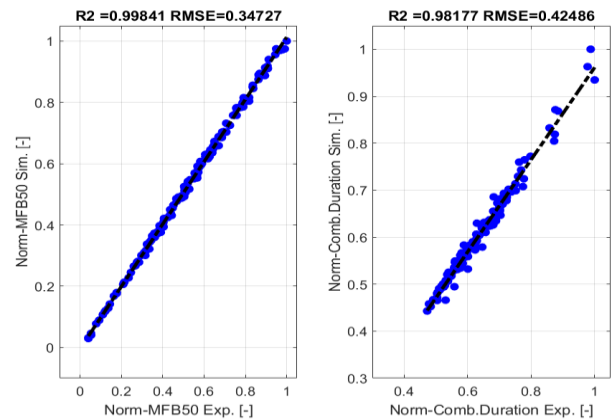


Figure 6. Correlation between experimental and simulated normalized MFB50 and normalized combustion duration for all the tested engine points.

The RMSE values displayed in the top of Figure 6 are not calculated with the normalized values but with the effective ones (expressed in

crank angle degrees), in order to provide a physical quantification of the results. R2 and RMSE indexes calculated for MFB50 and combustion duration further confirm the accuracy of the calibration process.

## Wiebe Function Parameters Analytical Model

The development of a simulation-oriented combustion model requires a detailed analysis of the Wiebe parameters E and D, for different operating conditions, in order to identify their trend w.r.t. engine speed, engine load and SA. Figure 7 shows values of coefficient E identified using the methodology described above, for all the engine points tested at 3000 RPM. The proposed analysis highlights that such parameter is strongly dependent on SA, and that such relationship can be effectively described using a polynomial of the first order. This trend is in agreement with the results shown by Lindstrom et al. [25], who demonstrated that the shape parameter (equivalent to the parameter E reported in Equation (3)) of the standard Wiebe law is higher when the SA increases. The authors explain that advancing the SA increases the ignition delay, due to the lower temperature and laminar burning velocity.

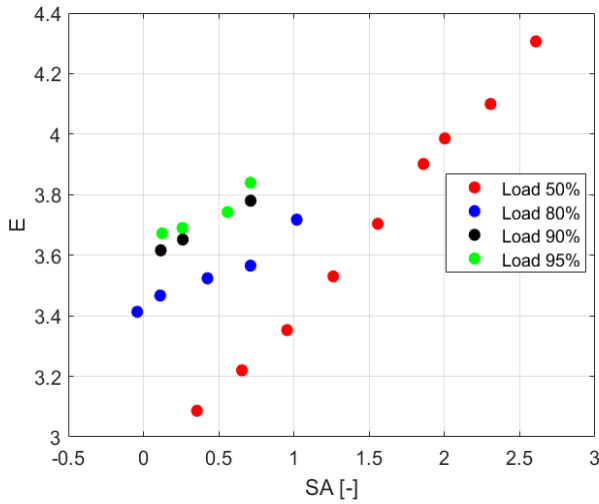


Figure 7. Trend of the coefficient E as a function of SA for all the engine conditions tested at 3000 RPM.

Considering the trend of coefficient E w.r.t. SA, the analytical model that represents such parameter on the entire engine operating field can be defined as a first-degree polynomial function, with SA as independent variable. The parameter under analysis varies also with the engine speed and load (as shown in Figure 7). Hence the gain and the offset of each linear function can be described as a polynomial of engine speed and load.

The analytical formulation of the parameter E may therefore be described by the following equations:

$$E = A_E SA + B_E \quad (6)$$

$$A_E = a_{00} + a_{10}X + a_{01}Y + a_{20}X^2 + a_{11}XY + a_{02}Y^2 \quad (7)$$

$$B_E = b_{00} + b_{10}X + b_{01}Y + b_{20}X^2 + b_{11}XY + b_{02}Y^2 + b_{21}X^2Y + b_{12}XY^2 + b_{03}X^3 \quad (8)$$

In equations (7) and (8) X and Y represent engine speed and load, respectively.

R2 values represent a statistical index that indicates the correlation quality between two or more variables. Thus, the polynomial degree for the equations that describe coefficients  $A_E$  and  $B_E$  are chosen as the highest value that ensures an increment of  $10^{-2}$  in terms of R2, in order to avoid overfitting. In the following table, the R2 values at the end of the fitting process of coefficients  $A_E$  and  $B_E$  are reported.

Table 3. R2 values given by the polynomial fitting used to model the Wiebe parameter E.

PARAMETER	R2
$A_E$	0.9136
$B_E$	0.9672

The high R2 values shown in Table 3 demonstrate that speed and load are the main influencing factors, whose effects may be captured with relatively low degree polynomials. Figure 8 shows the resulting trend of the interpolating surfaces, further highlighting that parameters of the first-degree polynomial described by Equation (6) are strongly related to engine speed and load.

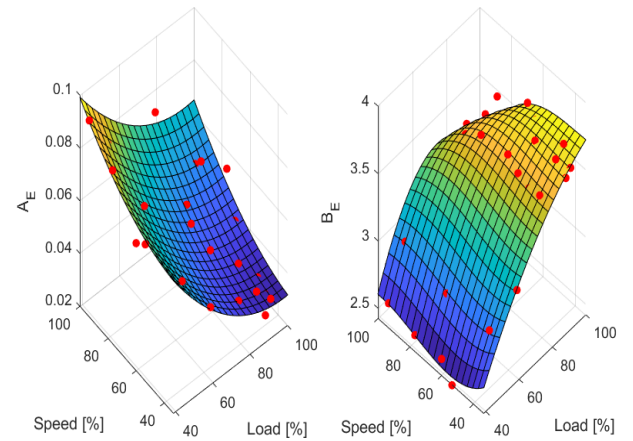


Figure 8. Polynomial functions used to describe the Wiebe coefficient E.

These trends can be analyzed further by observing the results of Figure 7, where it is shown an increasing trend with load of the considered index. As displayed in Figure 8, for the highest engine load, values correspond to the lowest values of the fitting function for the angular coefficient ( $A_E$ ) and vice versa for the offset ( $B_E$ ), which assumes numeric values that are two orders of magnitude higher than the first polynomial coefficient: this explains the general increasing trend with load of the coefficient E.

The method adopted to study the trend of the coefficient E was used also to investigate the dependency between the coefficient D and SA. In Figure 9, the trend of such coefficient is displayed, for the same engine points considered in Figure 7.

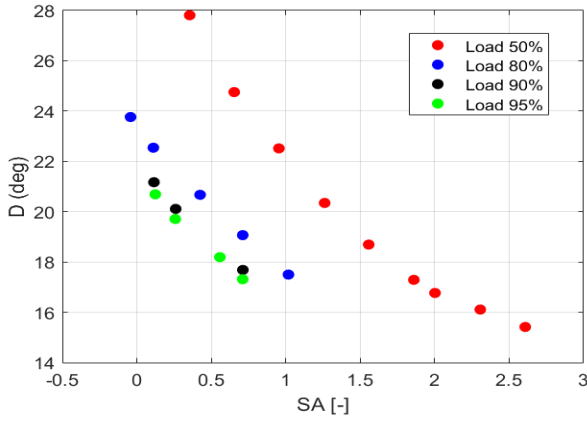


Figure 9. Trend of the D coefficient at 3000 RPM and different load values.

As well known, the higher the SA, the lower the combustion duration. Lindstrom et al. [25] state that this result depends on the faster rise of the pressure inside the combustion chamber achieved by advancing the spark timing. Trend of parameter D is parabolic w.r.t SA, thus Equation (9) may be defined as the corresponding mathematical model:

$$D = A_D SA^2 + B_D SA + C_D \quad (9)$$

where terms  $A_D$ ,  $B_D$  and  $C_D$  are described through polynomial functions. Polynomial order is decided through the same criteria on the R2 values (now collected in Table 4) used to define the relationship for coefficients  $A_E$  and  $B_E$ . The following equation defines the mathematical expression of parameter  $A_D$ , and also the other two coefficients can be represented with a polynomial equation of the same order (X and Y represent engine speed and load, respectively):

$$A_D = c_{00} + c_{10}X + c_{01}Y + c_{20}X^2 + c_{11}XY + c_{02}Y^2 + c_{21}X^2Y + c_{12}XY^2 + c_{03}Y^3 \quad (10)$$

Table 4. R2 values given by the polynomial fitting used to describe the Wiebe parameter D.

PARAMETER	R2
$A_D$	0.4603
$B_D$	0.9234
$C_D$	0.9573

The R2 values reported in Table 4 underline that the parameters  $B_D$  and  $C_D$  mainly depend on engine speed and load. The R2 value of the coefficient  $A_D$ , instead, shows that there is not a clear trend with respect to engine speed and load. This depends on the way with which tests are performed for high loads operating conditions: spark sweeps have been carried out over a narrower range of SA, due to knock limit on one side and an excessive exhaust temperature at turbine inlet on the other. This means that it is more difficult to characterize the parabolic trend for high load conditions. However, considering that the second-degree term ( $A_D$ ) assumes numeric values that are two orders of magnitude lower than the linear coefficient ( $B_D$ ) and three orders of magnitude lower than the offset

term ( $C_D$ ), the low R2 value found for the coefficient  $A_D$  does not introduce significant errors in the model. At the same time, it contributes to better capture the parabolic trend of coefficient D, that is evident especially at low loads.

The R2 value reported for the fitting of the term  $A_D$  also suggests that a constant value could, on paper, be considered as a valid solution instead of expressing it as a function of engine speed and load. Nevertheless, considering that a small error on Wiebe parameters strongly influences the simulated in-cylinder pressure, the authors chose to implement the corresponding polynomial equation.

The reliability of the analytical methodology for the calculation of Wiebe equation coefficients is further demonstrated by showing results of the calibration process for a GDI turbocharged V8 engine characterized by a central injector and a lateral spark plug. The same optimization routine based on the Equation (5) is applied for the calibration of the combustion model for such engine. Trends of coefficients and accuracy of results allow to state that the proposed approach can be extended to different engine and the calibration effort can be reduced, due to the same formulation of fitting polynomials. Data are referred to all the experimental tests available at 3000 RPM to carry out a direct and consistent comparison with Figure 7 and 9.

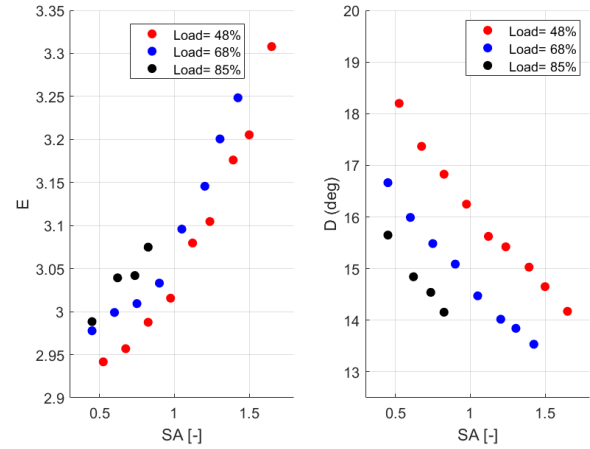


Figure 10. Trend of coefficient E and D for a GDI turbocharged engine with a central injector and lateral spark-plug.

Analysing this figure is clear that the trends of the Wiebe coefficients are in accord with the ones shown for the engine with the geometric characteristics shown in Table 1. Moreover, the numeric values are similar for the two engines.

Considering that for the engine with the central injector spark sweep tests are carried out for different engine speed and load conditions, it is possible to demonstrate that  $A_E$  and  $B_E$  have the same trend over the speed-load domain, according with values shown in Figure 8.

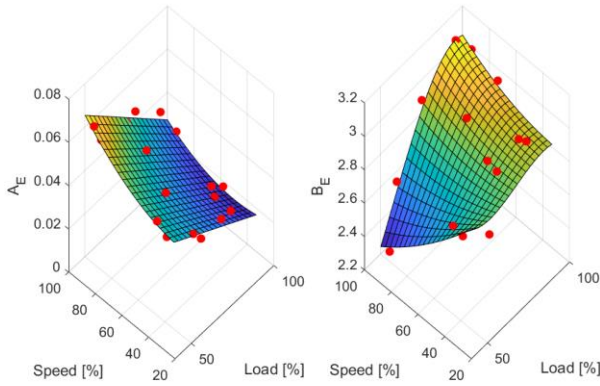


Figure 11. Polynomial functions used to describe the Wiebe coefficient E for the engine with the central injector and lateral spark plug.

Comparing these surfaces with those reported in Figure 8, numeric values of fitting polynomial coefficients are similar to the ones found for the other type of engine. Thus, it is possible to conclude that the approach exploited to model the Wiebe coefficients can be considered reliable and valid for all the engines, as demonstrated over the years for the Wiebe equation.

## 0-D Combustion Model Validation

In this section the performance of the polynomial combustion model is verified. A comparison is made between the experimental combustion indexes and the simulated ones, relating the correlation factors (R2 and RMSE) with the ones obtained for the combustion indexes calculated at the end of the calibration process.

During the validation phase, the highest importance is given to the MFB50 index because the simulated one is used as input for the polynomial transfer function that converts the simulated gas temperature at EVO into the value measured at the turbine inlet. Figure 12 shows normalized, experimental MFB50 values versus the normalized, simulated ones, highlighting the R2 and RMSE values (the latter expressed in crank angle degrees).

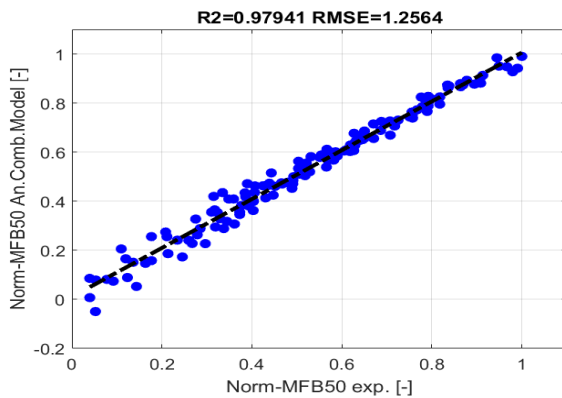


Figure 12. Correlation between normalized, experimental MFB50 values and the normalized ones calculated with polynomial Wiebe model.

When comparing the results reported in Figure 12 with the corresponding values calculated by applying the coefficient D and E calibrated for each engine point independently, the high level of

accuracy that the proposed approach guarantees can be highlighted. Indeed, R2 is decreased by 2% w.r.t. the value shown in Figure 6, and the RMSE is increased by 1 degree.

The same evaluation is performed for the maximum in-cylinder pressure value, which is a very important information that can be used in a combustion control system. Figure 13 displays the results for this variable: R2 is very close to 1 and the RMSE is around 3.3 bar. Such values demonstrate the extremely high accuracy of the proposed method even for this variable.

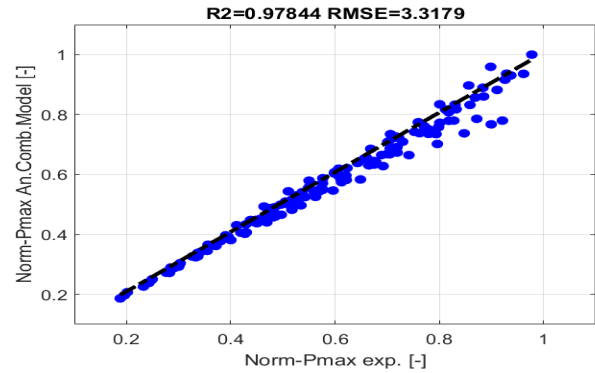


Figure 13. Correlation between experimental maximum in-cylinder pressure values and the ones calculated with polynomial Wiebe model.

## Temperature Conversion Model

Given a calibrated combustion model, the exhaust gas temperature at EVO within the combustion chamber can be calculated. This section discusses the definition of the analytical model that converts the output of the 0-D model into the gas temperature at the turbine inlet, that makes the final output of the complete model directly comparable with the TC output measured under steady-state conditions. In other words, this model calculates the difference between the modelled gas temperature at EVO and the experimental one at the turbine inlet. Its development was carried out by studying the trend of both this difference and the measured values w.r.t. engine speed and load axes and for a fixed MFB50. Such analysis is shown in Figure 14 for a MFB50 equal to 25° CA ATDC, where, on the left, red dots represent the normalized temperature difference between the simulated values at EVO and the TC output placed at the turbine inlet, while, the latter are normalized and reported on the right.

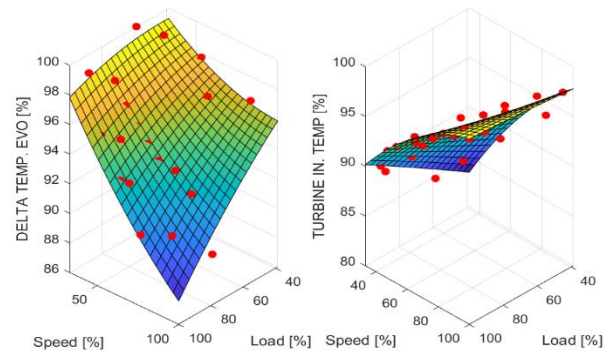


Figure 14. Normalized trend of the difference between simulated EVO temperatures and experimental inlet turbine ones (on the left) and experimental temperatures at turbine inlet (on the right) as function of engine speed and load, for a fixed value of MFB50 = 25° ATDC.

The calculated values and the polynomial fit show a smooth trend versus engine speed and load for both variables. The trend reported on the left is in agreement with values shown on the right, and this confirms that at the turbine inlet the highest temperature is achieved for the highest engine speed values (i.e., when the temperature difference is minimum). This is due to the increasing thermal power released in the exhaust manifold. It is important to highlight that the experimental exhaust temperatures are strongly affected by the actuated lambda value, that is equal to the calibrated value for all the tests. This means that the decreasing trend, shown in the left graph of Figure 14, would be even more pronounced with a stoichiometric mixture on the entire engine operating field.

The approach followed for the development of the temperature transfer function is similar to the method applied for the analytical definition of the coefficients D and E. The difference between simulated EVO temperatures and the experimental exhaust steady-state at turbine inlet (DELTA\_T) was investigated as a function of simulated MFB50 for each engine point. In Figure 15, the results for the engine points at 3000 RPM are shown. The values are reported in physical units but normalized w.r.t. minimum one. By analyzing the reported data, it is possible to model the trend of the difference between the simulated EVO temperatures and the experimental ones measured at turbine inlet versus the simulated MFB50. The resulting trend suggests that advancing the combustion towards the expansion phase, the temperature difference between EVO and turbine inlet increases linearly, with a smaller dependence on engine load.

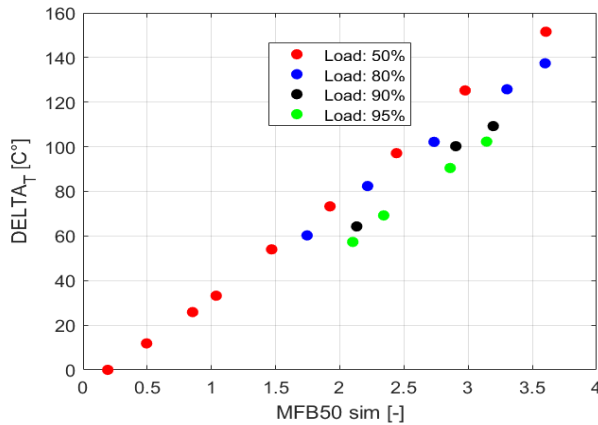


Figure 15. Trend of the difference between the simulated EVO temperature and the measured one within the exhaust manifold as a function of simulated MFB50 for each spark sweep test at 3000 RPM.

The proposed analytical model is comparable to the one defined in Equation (6), in which the independent variable SA is replaced by the simulated MFB50. Coefficients  $A_T$  and  $B_T$  (as  $A_E$  and  $B_E$ ) can be defined as a function of engine speed and load, considering the maximum R2 value achieved during the fitting process of the gains and offsets calculated for each engine point independently. R2 values are collected in Table 5.

Table 5. R2 values given by the polynomial function used to describe the difference between simulated EVO temperatures and exhaust measured ones.

PARAMETER	R2
$A_T$	0.9621
$B_T$	0.7765

## Temperature Conversion Model Validation

The complete semi-physical simulation-oriented model composed of Wiebe parameters analytical model and the polynomial transfer function for the exhaust temperature is eventually validated. The model shown in Figure 2 is fed with experimental steady-state data of engine speed, load, and SA of each engine point tested during spark sweeps. The model outputs are compared with the experimental exhaust temperatures measured by the TC under the same steady-state conditions. In the left subplot of Figure 16, the percentage error (referred to Celsius degrees) between the experimental and the simulated values is displayed and the high accuracy of the model is confirmed. Indeed, all the modelling errors are included in a range of  $\pm 2\%$ , with a mean absolute error of 0.53 %. In the right subplot the correlation between experimental and calculated temperature is shown and the R2 and RMSE (units are Celsius degrees) are reported.

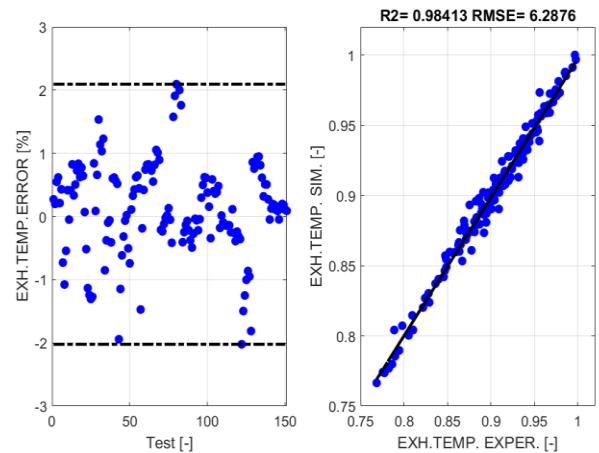


Figure 16. Percentage error and correlation graph between experimental and simulated exhaust temperatures calculated by the 0-D simulation-oriented model.

The results of the model shown in Figure 16 have to be analysed considering that TC measurement is taken as reference. Indeed, such measurement is affected by the conduction and radiation between TC and pipe wall and dynamics effects related to the measurement chain. Papaioannou et al. [26] demonstrate that using standard 3 mm sheathed thermocouple the average exhaust gas temperature measured under steady-state conditions can be underestimated of 40 °C w.r.t. the one measured with fast-response probes, which can better capture temperature oscillations during the engine cycle. Considering 40 °C a baseline error for a 3 mm sheathed thermocouple, the RMSE value reported in Figure 16, which is about six times lower than the considered error, demonstrates the high accuracy of the model w.r.t. the available experimental data.

## Control-Oriented Model

The simulation-oriented model cannot be implemented in a RT application, because Equation (2) needs to be integrated in the angular domain in order to calculate the temperature and pressure profiles within the combustion chamber. At the same time, the proposed model would be useful to support a new combustion phase control system by predicting inlet turbine temperature values, thus limiting the current intervention of load reduction or mixture enrichment strategies.

The definition of some synthetic indexes used as inputs of the Wiebe model is needed to make the complete model suitable to be implemented in a RT control strategy. Therefore, an analytical approach is applied to calculate the MFB50 and the EVO gas temperature to obtain the gas temperature at the turbine inlet under steady state conditions. It is important to highlight that the development of the control-oriented model is carried out without modifying the polynomial models of Wiebe parameters and the temperature conversion function.

In the control-oriented model, the analytical approach used to calculate the MFB50 comes from GT-Power library [6] and it is directly related to the Wiebe function defined by Equation (3):

$$SOC = MFB50 - \frac{D BMC_{E+1}^{\frac{1}{E+1}}}{BEC_{E+1}^{\frac{1}{E+1}} - BSC_{E+1}^{\frac{1}{E+1}}} \quad (11)$$

Where  $BMC = -\ln(0.5)$ . Considering that the combustion model was calibrated with the hypothesis  $SOC = SA$ , Equation (11) can be easily inverted to calculate the MFB50, exploiting the analytical models of E and D defined by Equation (6) and (9) respectively. To demonstrate the validity of this approach, in Figure 17 the difference between the MFB50 values calculated from the simulated heat release and those estimated by inverting Equation (11) is shown.

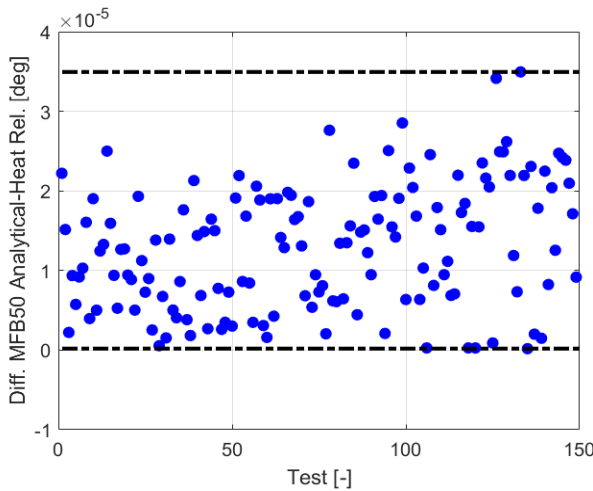


Figure 17. Difference between the MFB50 calculated with the analytical approach and the same parameter calculated with the simulated heat release.

The approach used to implement the analytical function which allows to calculate the gas temperature at EVO without solving Equation (2) is equivalent to the method developed for the temperature conversion function. This means that for each tested engine point (for fixed speed and load), the trend of the gas temperature at EVO can be described through a linear function with simulated MFB50 as the independent variable. Indeed, the mathematical formulation is similar to (6) and the polynomial coefficients  $A_{T1}$  and  $B_{T1}$  (corresponding respectively to  $A_E$  and  $B_E$  of Equation (6)) can be modelled with two equations equivalent to (7). Hence, the scheme of the 0-D simulation-oriented model (reported in Figure 3) can be updated with the two analytical models described above. Figure 18 shows the representation of the resulting control-oriented model.

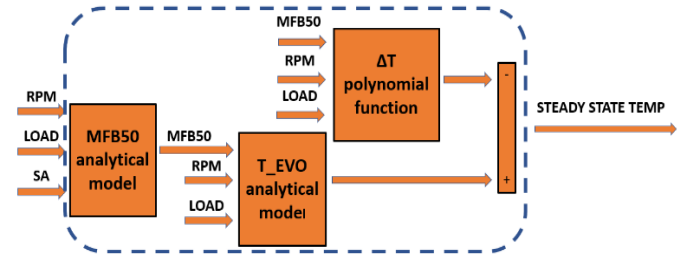


Figure 18. Layout of the control-oriented model. As for the semi-physical one, the inputs are engine speed, load and spark advance.

The exhaust temperatures calculated with the control-oriented model can be compared to the experimental values for the same operating conditions (engine speed, load and SA). Considering the following figure, it is possible to demonstrate the accuracy of the global analytical model. The exhaust temperature percentage error is within a  $\pm 3\%$  range, with a mean absolute error of 0.81 %. It is slightly worse than results of the semi-physical model, but the error values are absolutely deemed to be acceptable considering the overall accuracy over the entire engine operating range.

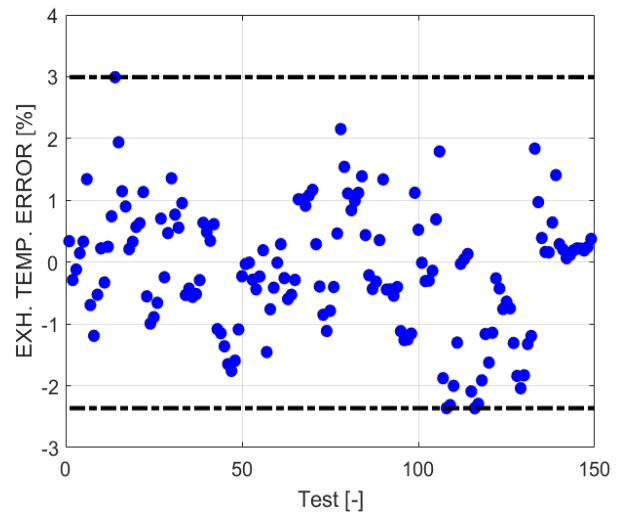


Figure 19. Percentage error between experimental and simulated exhaust temperatures with the use of the control-oriented model.

## Control Oriented Model Dynamic Validation

The validation under transient conditions is carried out by feeding the control-oriented model with experimental profiles of engine speed, load, and SA which were recorded during dedicated tests. In the first one, engine speed is kept constant while load and SA are varied. The second test is more general because all the three input parameters are changed. It is important to highlight that lambda is always equal to the mapped values, so no effects of mixture quality variations are present. Both tests are performed on engine operating conditions particularly stressful for the turbine. In this way, the key role of an accurate exhaust temperature model can be demonstrated. Moreover, engine points not included in the database used for the calibration process are tested to further validate the accuracy of the calibration process. For the validation under transient conditions the control-oriented model was coupled with the real-time thermocouple model described and calibrated in a previous work by the authors [20]. It is

important to mention that the focus of this paragraph is mainly to validate the model under transient conditions, and the TC model is useful just to have an output signal directly comparable with the actual TC reading. Since the final objective of the control-oriented model is that to be implemented in a control strategy for the RT estimation and management of the gas temperature at the turbine inlet, the application of the TC dynamics model can be excluded from the final implementation, due to the underestimation of the gas temperature under transient conditions. When the gas temperature changes instantaneously, the behavior of the TC output is initially characterized by a fast response, followed by a slower transient to reach steady state. The TC time constant and the gas mixing within the exhaust manifold cause the faster part of the dynamics, while conduction and radiation phenomena are responsible for the slower one and they practically act like two coupled first-order systems. The approach used to reproduce such trend is based on the algebraic sum of the output of two different filters, that were implemented in the form of two weighted averages. The one with the lower weight for the old value corresponds to the fast filter, and the one with the higher weight corresponds to the slower one. The simplified block in the following figure shows how the two models are coupled to simulate the TC signal.

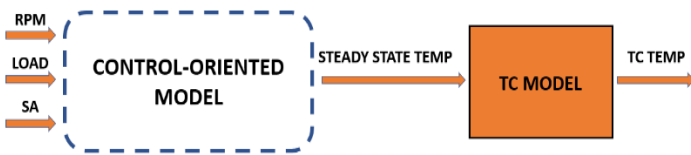


Figure 20. Layout of the model used for the validation under transient conditions.

In Figure 21 the experimental profiles of engine speed, load, SA, and lambda of test n.1 are reported.

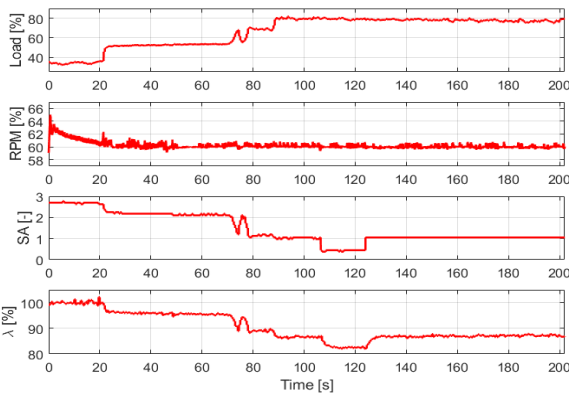


Figure 21. Experimental profiles of engine speed, load, SA and  $\lambda$  used for test n. 1.

In Figure 22 the simulated exhaust temperature at turbine inlet and MFB50 are compared with the experimental values. The experimental MFB50 profile shown in Figure 22 is determined as the mean value between all the cylinders. Analyzing this figure, it is possible to verify the accuracy of the model. Indeed, the percentage error is included within a range of  $\pm 2\%$ .

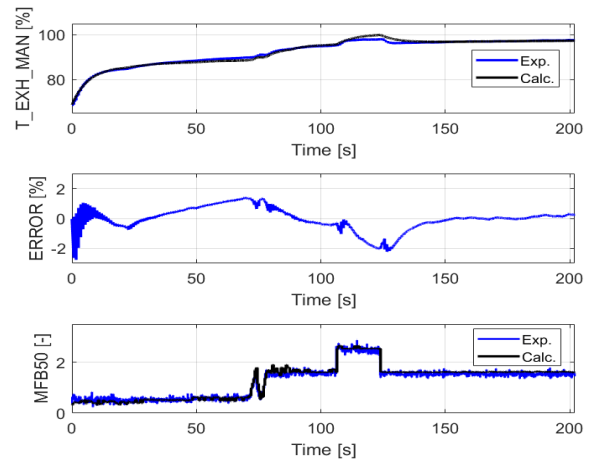


Figure 22. Performance of the control-oriented model under transient conditions (test n. 1).

The error of MFB50 model can be studied even with a statistical approach, considering that the simulated signal can not reproduce cycle-to-cycle variation. In Figure 23 the Gaussian Probability Density Function (PDF) of the error between experimental and simulated MFB50 is shown, highlighting the mean value and the standard deviation in the title.

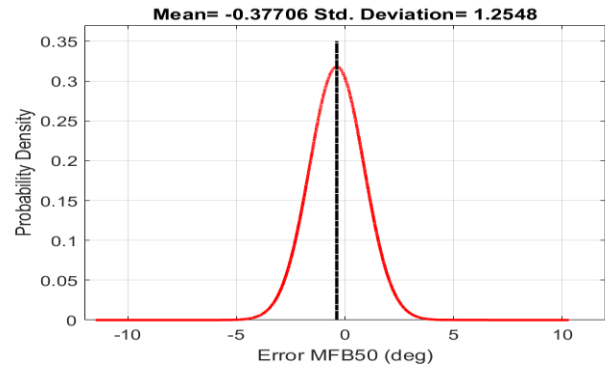


Figure 23. PDF of the error between experimental and simulated MFB50 (test n.1).

In Figure 24, the experimental profiles of engine speed, load, and SA of test n.2 are shown, and in Figure 25 the corresponding results are presented. Such test is characterized by a speed variation between 40 and 80% and a load variation between 60 and 90%, touching several engine points non included in the calibration database. In other words, results achieved with this test are a complete demonstration of modelling approach reliability on a wide range of the engine operating filed and, in particular, on the area in which exhaust gas temperature forces manufacturers to calibrate lambda values lower than 1.

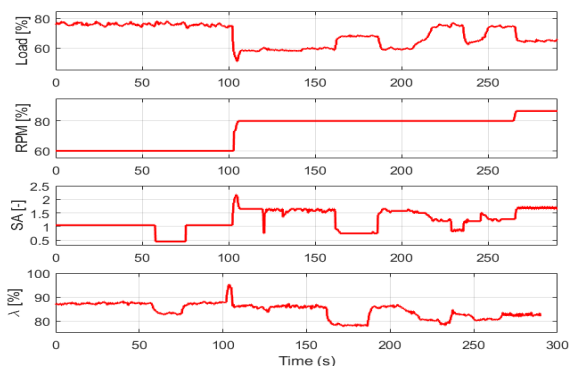


Figure 24. Experimental profiles of engine speed, load and SA used for test 2.

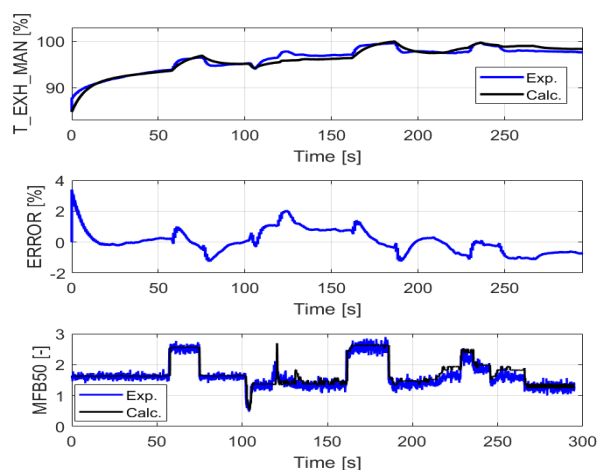


Figure 25. Performance of the control-oriented model under transient conditions (test 2).

Also, for this test the performances of the MFB50 model can be studied with a statistical approach as shown in Figure 26.

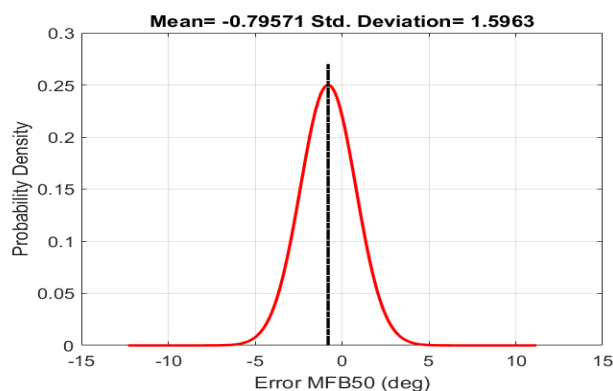


Figure 26. PDF of the error between experimental and simulated MFB50 (test n.2).

Considering results achieved for transient tests, it is possible to conclude that the control-oriented model can calculate the exhaust gas temperature with an accuracy between  $\pm 2\%$ , while the MFB50 is

simulated with an average error lower than  $1^\circ$  and a 95% confidence interval of about  $\pm 3^\circ$ , on the whole engine operating field characterized by middle-high speed and load.

## Conclusion and Future Works

Both a semi-physical, simulation-oriented model and a real-time, control-oriented model for the exhaust gas temperature estimation have been developed and critically analyzed. The semi-physical, Wiebe-based model uses a zero-dimensional approach to estimate the heat release curve and the in-cylinder pressure curve during the closed-valve portion of the engine cycle. The development of the combustion model is carried out by exploiting a novel calibration procedure of Wiebe function parameters compatible with RT execution of the final model. For the exponent E it is demonstrated that the values can be described with a first-degree polynomial as a function of SA for each engine point. The same analysis is carried out for the combustion duration D for which a parabolic function is the optimal equation to describe the SA dependency, according to the experimental trend.

The other important part of the semi-physical simulation-oriented model is the temperature conversion function that converts exhaust gas temperature at EVO into the turbine inlet one. Its development is carried out applying the same method used for Wiebe parameters. The trend identified is a first-degree polynomial with MFB50 as independent variable.

The final objective of this work was the development of a control-oriented model for the estimation of the exhaust gas temperature, suitable to be implemented in the ECU, and directly based on the models introduced in the 0-D simulation-oriented model. In order to calculate the exhaust gas temperature, a RT-compatible analytical method was finally chosen, due to the high computational effort needed to solve a pure 0-D physical method. The control-oriented model is validated under steady-state conditions, achieving results comparable to those of the semi-physical model, with an error within  $\pm 3\%$  for all tested points. The validation under transient conditions is then performed with two different tests, with which it is demonstrated that the control-oriented model can simulate the exhaust gas temperature with an accuracy of  $\pm 2\%$  and the MFB50 with an average error lower than  $1^\circ$  and a 95% confidence interval of about  $\pm 3^\circ$  on a wide portion of engine operating field, touching points not included in the calibration database.

Future developments of the model will deal with the introduction of the lambda dependency to count the effects of all the control actuations which affect the exhaust gas temperature.

## References

1. Zhao, F., "Technologies for Near-Zero-Emission Gasoline-Powered Vehicles", SAE International, 2006, Warrendale, USA, ISBN13: 9780768014617
2. Cavina, N., Mancini, G., Corti, E., Moro, D. et al., "Thermal Management Strategies for SCR After Treatment Systems," SAE Technical Paper 2013-24-0153, 2013, <https://doi.org/10.4271/2013-24-0153>.
3. Fu, H., Chen, X., Shilling, I., and Richardson, S., "A One-Dimensional Model for Heat Transfer in Engine Exhaust Systems," SAE Technical Paper 2005-01-0696, 2005, <https://doi.org/10.4271/2005-01-0696>.

4. Fulton, B., Van Nieuwstadt, M., Petrovic, S., and Roettger, D., "Exhaust Manifold Temperature Observer Model," SAE Technical Paper 2014-01-1155, 2014, <https://doi.org/10.4271/2014-01-1155>.
5. Martin, D. and Rocci, B., "Virtual Exhaust Gas Temperature Measurement," SAE Technical Paper 2017-01-1065, 2017, <https://doi.org/10.4271/2017-01-1065>.
6. Gamma Technology Inc., "GT-ISE 2018 Documentation", 2018.
7. Borg, J. and Alkidas, A., "Investigation of the Effects of Autoignition on the Heat Release Histories of a Knocking SI Engine Using Wiebe Functions," SAE Technical Paper 2008-01-1088, 2008, <https://doi.org/10.4271/2008-01-1088>.
8. Saad, C., maroteaux, F., Millet, J., and Aubertin, F., "Combustion Modeling of a Direct Injection Diesel Engine Using Double Wiebe Functions: Application to HiL Real-Time Simulations," SAE Technical Paper 2011-24-0143, 2011, <https://doi.org/10.4271/2011-24-0143>.
9. Malbec, L., Le Berr, F., Richard, S., Font, G. et al., "Modelling Turbocharged Spark-Ignition Engines: Towards Predictive Real Time Simulators," SAE Technical Paper 2009-01-0675, 2009, <https://doi.org/10.4271/2009-01-0675>.
10. Ravaglioli, V., Moro, D., Serra, G., and Ponti, F., "MFB50 On-Board Evaluation Based on a Zero-Dimensional ROHR Model," SAE Technical Paper 2011-01-1420, 2011, <https://doi.org/10.4271/2011-01-1420>.
11. Ranuzzi, F., Cavina, N., Brusa, A., De Cesare, M. et al., "Development and Software in the Loop Validation of a Model-based Water Injection Combustion Controller for a GDI TC Engine," SAE Technical Paper 2019-01-1174, 2019, <https://doi.org/10.4271/2019-01-1174>.
12. Brusa, A., Cavina, N., Rojo, N., Cucchi, M. et al., "Development and Validation of a Control-Oriented Analytic Engine Simulator," SAE Technical Paper 2019-24-0002, 2019, <https://doi.org/10.4271/2019-24-0002>.
13. GT-SUITE, Engine Performance Application Manual, Version 2018
14. Egan, D., Koli, R., Zhu, Q., and Prucka, R., "Use of Machine Learning for Real-Time Non-Linear Model Predictive Engine Control," SAE Technical Paper 2019-01-1289, 2019 <https://doi.org/10.4271/2019-01-1289>.
15. Eriksson, L., "Mean Value Models for Exhaust System Temperatures," SAE Technical Paper 2002-01-0374, 2002, <https://doi.org/10.4271/2002-01-0374>.
16. Papaioannou, N., Leach, F., and Davy, M., "Effect of Thermocouple Size on the Measurement of Exhaust Gas Temperature in Internal Combustion Engines," SAE Technical Paper 2018-01-1765, 2018, <https://doi.org/10.4271/2018-01-1765>.
17. Muric, K., Tunestal, P., and Stenlaas, O., "A Fast Crank Angle Resolved Zero-Dimensional NO<sub>x</sub> Model Implemented on a Field-Programmable Gate Array," *SAE Int. J. Engines* 6(1):246-256, 2013, <https://doi.org/10.4271/2013-04-0344>.
18. Kar, K., Roberts, S., Stone, R., Oldfield, M. et al., "Instantaneous Exhaust Temperature Measurements Using Thermocouple Compensation Techniques," SAE Technical Paper 2004-01-1418, 2004, <https://doi.org/10.4271/2004-01-1418>.
19. C. D. Henning and R. Parker, "Transient response of an intrinsic thermocouple", *J. Heat Transfer*. May 1967, 89(2): 146-152, <https://doi.org/10.1115/1.3614337>.
20. Brusa, A., Mecagni, J., Cavina, N., Corti, E. et al., "Development and Experimental Validation of a Control-Oriented Empirical Exhaust Gas Temperature Model," SAE Technical Paper 2020-24-0008, 2020, <https://doi.org/10.4271/2020-24-0008>.
21. Gopujkar, S., Worm, J., and Robinette, D., "Methods of Pegging Cylinder Pressure to Maximize Data Quality," SAE Technical Paper 2019-01-0721, 2019, <https://doi.org/10.4271/2019-01-0721>.
22. Loganathan, S., Murali Manohar, R., Thamaraikannan, R., Dhanasekaran, R. et al., "Direct Injection Diesel Engine Rate of Heat Release Prediction using Universal Load Correction Factor in Double Wiebe Function for Performance Simulation," SAE Technical Paper 2011-01-2456, 2012, <https://doi.org/10.4271/2011-01-2456>.
23. McBride, B.J., Gordon, S., Reno, M.A., "Coefficients for Calculating Thermodynamic and Transport Properties of Individual Species", NASA Technical Memorandum 4513
24. Matlab Documentation, The MathWorks, 2020, <https://www.mathworks.com/>
25. Lindström, F., Ångström, H., Kalghatgi, G., and Möller, C., "An Empirical SI Combustion Model Using Laminar Burning Velocity Correlations," SAE Technical Paper 2005-01-2106, 2005, <https://doi.org/10.4271/2005-01-2106>.
26. Papaioannou, N., Leach, F., and Davy, M. (June 30, 2020). "Improving the Uncertainty of Exhaust Gas Temperature Measurements in Internal Combustion Engines." *ASME. J. Eng. Gas Turbines Power*. July 2020; 142(7): 071007. <https://doi.org/10.1115/1.4047283>
27. C. D. Henning and R. Parker, "Transient response of an intrinsic thermocouple", *J. Heat Transfer*. May 1967, 89(2): 146-152, <https://doi.org/10.1115/1.3614337>.
28. Gat, U., Kammer, D., Hahn, O. J., "The effect of temperature dependent properties on transient measurement with intrinsic thermocouple", *International Journal of Heat and Mass Transfer*, vol.18, Dec. 1975, p 1337-1342.
29. Cavina, N., Migliore, F., Carmignani, L., and Di Palma, S., "Development of a Control-Oriented Engine Model Including Wave Action Effects," SAE Technical Paper 2009-24-0107, 2009, <https://doi.org/10.4271/2009-24-0107>.
30. Millo, F., Di Lorenzo, G., Servetto, E., Capra, A. et al., "Analysis of the Performance of a Turbocharged S.I. Engine under Transient Operating Conditions by Means of Fast Running Models," *SAE Int. J. Engines* 6(2):968-978, 2013, <https://doi.org/10.4271/2013-01-1115>.
31. Boiarciuc, A. and Floch, A., "Evaluation of a 0D Phenomenological SI Combustion Model," SAE Technical Paper 2011-01-1894, 2011, <https://doi.org/10.4271/2011-01-1894>.
32. Dekraker, P., Barba, D., Moskalik, A., and Butters, K., "Constructing Engine Maps for Full Vehicle Simulation Modeling," SAE Technical Paper 2018-01-1412, 2018, <https://doi.org/10.4271/2018-01-1412>.
33. Finesso, R., Spessa, E., Yang, Y., Conte, G. et al., "Neural-Network Based Approach for Real-Time Control of BMEP and MFB50 in a Euro 6 Diesel Engine," SAE Technical Paper 2017-24-0068, 2017, <https://doi.org/10.4271/2017-24-0068>.
34. Brusca, S., Lanzafame, R., and Messina, M., "A Combustion Model for ICE by Means of Neural Network," SAE Technical Paper 2005-01-2110, 2005, <https://doi.org/10.4271/2005-01-2110>.

## Definitions/Abbreviations

ATDC	After Top Dead Center
------	-----------------------

<b>BTDC</b>	Before Top Dead Center	<b>TC</b>	Thermocouple
<b>CA</b>	Crank Angle	<b>UEGO</b>	Universal Exhaust Gas Oxygen Sensor
<b>CI</b>	Compression Ignition	<b>WOT</b>	Wide Open Throttle
<b>ECU</b>	Engine Control Unit		
<b>EVO</b>	Exhaust Valve Opening		
<b>FPGA</b>	Field Programmable Gate Array		
<b>GDI</b>	Gasoline Direct Injection		
<b>HiL</b>	Hardware in the Loop		
<b>IVC</b>	Intake Valve Closing		
<b>MA</b>	Moving Average		
<b>MFB10</b>	10% of Mass Fraction Burned		
<b>MFB50</b>	50% of Mass Fraction Burned		
<b>MFB90</b>	90% of Mass Fraction Burned		
<b>MIMS</b>	Mineral-Insulated-Metal-Sheathed		
<b>NN</b>	Neural Network		
<b>PDE</b>	Partial Differential Equation		
<b>PDF</b>	Probability Density Function		
<b>R2</b>	R-Square		
<b>RMSE</b>	Root Mean Square Error		
<b>RT</b>	Real Time		
<b>RTD</b>	Resistance Temperature Detector		
<b>SA</b>	Spark Advance		
<b>SI</b>	Spark Ignition		
<b>SiL</b>	Software in the Loop		
<b>SOC</b>	Start of Combustion		